Cell Communication and Signaling

RESEARCH Open Access

Inflammatory macrophages drive smooth muscle dedifferentiation via YAP signaling in murine deep vein thrombosis

Huan Yang[1], Ting Zhou[1*], Jooyong Kim[1] and Bo Liu[1*]

Abstract

Background Deep vein thrombosis (DVT) is a common clinical problem characterized by the formation of blood clots in deep veins. The contribution of venous smooth muscle cells (SMCs) to the onset of DVT, particularly the mechanisms driving their phenotypic changes, remains poorly understood.

Methods We employed a murine stasis model of DVT via inferior vena cava (IVC) ligation in both male and female mice. Single-cell RNA sequencing (scRNA-seq) was used to analyze the cellular and transcriptomic landscape of the vein wall 24 h post-ligation. To investigate cellular crosstalk, we utilized in vitro systems where primary mouse aortic SMCs and human saphenous vein SMCs were treated with conditioned media from inflammatory myeloid cells. The effects on SMC phenotype and signaling were assessed using bulk RNA-seq, Western blotting, RT-qPCR, and functional assays.

Results scRNA-seq analysis revealed that DVT induction promotes a rapid inflammatory response characterized by neutrophil influx and a shift in SMCs from a contractile to a synthetic phenotype in both sexes. Infiltrating myeloid cells were identified as a primary source of signaling to SMCs. In vitro, conditioned media from inflammatory macrophages was sufficient to suppress SMC contractile gene expression and function. Mechanistically, this effect was linked to the inhibition of the Hippo pathway effector YAP, evidenced by increased YAP phosphorylation (S127/S397) and a subsequent reduction of total YAP protein in SMCs. We identified macrophage-derived IL-1β as a key ligand that mimics these effects. Importantly, pharmacological activation of YAP rescued contractile gene expression in SMCs exposed to the inflammatory macrophage secretome.

Conclusions Our findings demonstrate that SMC dedifferentiation occurs early in DVT, driven by inflammatory macrophage-mediated suppression of YAP signaling. This study uncovers a critical macrophage-SMC crosstalk mechanism in early DVT pathogenesis and highlights YAP as a potential therapeutic target to preserve vein wall integrity and prevent long-term complications.

Keywords Deep vein thrombosis, smooth muscle cells, inflammation, YAP signaling

*Correspondence:
Ting Zhou
ting.zhou@wisc.edu
Bo Liu
bliu24@wisc.edu
[1]Department of Cell and Regenerative Biology, School of Medicine and Public Health, University of Wisconsin-Madison, 1111 Highland Avenue, Madison, WI 53705, USA

Background

Deep vein thrombosis (DVT), the formation of blood clots in deep veins, is a common vascular disease that can lead to severe complications including pulmonary embolism. DVT can also cause post-thrombotic syndrome, a condition characterized by long-term vein wall damage and remodeling [1, 2]. The pathophysiology of DVT involves complex interactions among coagulation factors, blood cells, and the vein wall [3]. While the contribution of the endothelium is well-recognized, the role of smooth muscle cells (SMCs)—another major cellular constituent of the vein wall—remains less understood [3]. Due to limited access to affected vein wall tissue from patients, investigations into venous remodeling rely heavily on animal models, including the full or partial ligation of the inferior vena cava (IVC)—referred to as stasis and stenosis models, respectively—as well as ferric chloride and electrolytic injury models [4, 5]. Using the stasis model of IVC ligation in male mice, our previous single-cell RNA sequencing (scRNA-seq) study characterized the cellular and molecular signatures of the vein wall 24 h after thrombosis [6]. We observed a dramatic shift in the cellular landscape, dominated by neutrophil infiltration and a reduction in vascular cells. Notably, SMCs displayed clear transcriptomic changes indicative of dedifferentiation, including the downregulation of contractile genes. However, the mechanisms driving this process and whether a similar phenotypic shift occurs in female mice remain unknown.

The contribution of SMC phenotypic change to vascular pathophysiology has been reported in the context of arterial diseases including atherosclerosis, restenosis, and aortic aneurysm [7–9]. Experimental evidence from linage tracing combined with scRNA-seq showed that SMCs can shift from a differentiated contractile phenotype to other functional phenotypes, such as proliferation, migration, inflammation, or fibroblast-like [7, 8]. Multiple transcription factors and co-factors as well as epigenetic mechanisms have been shown to regulate the transition of SMC from a contractile to a de-differentiated state in the context of arterial disease [10, 11]. While the underlying molecular mechanisms may vary depending on disease or the nature of injury, diminished expression of contractile genes including *Acta2*, *Myh11*, and *Cnn1* is a common characteristic of phenotypic shift [7, 8].

In this study, we used scRNA-seq to characterize the SMC phenotypic shift in both male and female mice in the stasis DVT model. In addition, we explored how inflammatory cells influence SMC dedifferentiation using an in vitro cell-cell communication system.

Methods

Human saphenous vein smooth muscle cells

The human saphenous vein SMCs was a generous gift from Dr. Xiaochun Long at Augusta University. Cells were prepared by the cell culture core in the Department of Molecular and Cellular Physiology at Albany Medical College as previously described [12]. Discarded human saphenous vein tissues were obtained from patients undergoing coronary artery bypass grafting (CABG). Sample collection and related experiments were exempt from human subjects' restrictions by the Institutional Review Board at Albany Medical College (IRB#3793). Cells were maintained in human vascular SMC basal medium (M231500, ThermoFisher Scientific), supplemented with smooth muscle growth supplement (SMGS, S00725, ThermoFisher Scientific), at 37 °C and 5% CO_2.

Animal studies and DVT model

All animal procedures were conducted under the approval of the University of Wisconsin—Madison Animal Care and Use Committee (Protocol #M005792). All experiments used 8- to 12-week-old, weight-matched male or female C57BL/6J mice (The Jackson Laboratory, Stock #000664).

The mouse stasis model of DVT was induced through inferior vena cava (IVC) ligation [6]. Mice were anesthetized with 5% isoflurane and maintained on 2.5% isoflurane thereafter. 0.6 mg/kg buprenorphine was administered subcutaneously for pain management before a midline laparotomy was performed. The IVC was exposed, and its back and side branches were respectively cauterized and ligated. The IVC was then fully ligated with 7/0 polypropylene suture just below the left renal vein. For control animals, a sham surgery consisting of vessel dissection without ligation was performed.

Sample collection and preparation

Mice were euthanized 6–24 h after surgery. For histological studies, the IVC with the thrombus was collected, embedded, and sectioned for immunofluorescent staining.

For scRNA-seq, IVCs were carefully dissected from adjacent tissues and any intraluminal thrombus, and subjected to a two-step enzymatic digestion to generate single-cell suspensions. Single-cell suspensions from 6 DVT-adjacent IVCs were pooled to generate the experimental sample, and suspensions from 6 sham IVCs were pooled to generate the control sample. From each pooled sample, 10,000 cells were loaded using the 10x Genomics Chromium platform with the Single Cell 3' v3.1 Reagent Kit to construct libraries. Libraries were then sequenced on an Illumina NovaSeq X Plus flowcell using a 2 × 150 bp sequencing reaction, targeting > 90,000 reads per cell.

For bulk RNA-seq, primary SMCs were treated with conditioned media, harvested, and RNA was extracted. The extracted RNA was then used to synthesize cDNA and prepare a library using an Illumina Stranded mRNA Prep kit, following the manufacturer's instructions. The cDNA library was then subjected to Illumina NovaSeq X Plus sequencing with the settings of 2 × 150 bp and 50 million reads per sample.

Bioinformatic analysis

For scRNA-seq, raw sequencing reads were aligned to the mouse reference genome (mm10) and quantified using Cell Ranger Count (v6.1.2). The resulting data was analyzed with the OmicVerse package (v1.7.1) [13] on the Python 3.11 platform. After removing low-quality cells, data was normalized and integrated across samples. Cell clusters were identified, and their identities were confirmed by identifying enriched genes and examining the expression of known canonical markers.

Differential expression analysis between the DVT and sham groups was performed using the MAST package, with differentially expressed genes (DEGs) identified based on a log2 fold change > 0.25 and a Bonferroni adjusted p-value < 0.0001. These DEGs were then used for pathway enrichment analysis with clusterProfiler (v4.16). To investigate cellular crosstalk, cell-cell communication networks were inferred using CellChat (v2.1), with a significance threshold of $p < 0.05$.

For bulk RNA-seq analysis, salmon (version 1.10.1) [14] was employed to quantify transcript levels. DESeq2 was used to normalize the counts and identify differentially expressed genes (DEGs). Subsequently, these DEGs were utilized for pathway enrichment analysis using clusterProfiler. Ligand activities mediating BMDM-SMC intercellular communication were predicted by using the nichenetr package (v2.2.0) [15]. BMDM bulk RNA-seq datasets were downloaded from GEO (GSE103958).

Immunofluorescent staining

Cell or tissue sections were fixed with 4% PFA, permeabilized with 0.1% Triton X-100, and blocked with 3% donkey serum. Sections were incubated at 4 °C overnight in 0.3% BSA containing primary antibodies: FITC anti-α-smooth muscle actin (ab8211, Abcam; 1:500), anti- Phospho-YAP (Ser127) (13008, Cell Signaling Technology; 1:100), anti-YAP (14074, Cell Signaling Technology, 1:100), anti-Calponin-1 (sc-58707, Santa Cruz, 1:100), anti-SM22α (ab14106, Abcam; 1:100). After several washes with PBS, sections were incubated with Alexa Fluor 488- or Alexa Fluor 594-conjugated secondary antibodies for 1 h at room temperature. Negative control slides were stained with secondary antibody only. DAPI-containing mounting media (GBI Labs, Catalog #E19-100) was used as a counterstain. Images were acquired with a Nikon A1RS confocal microscope system and analyzed using Fiji software.

Isolation and culture of primary mouse aortic smooth muscle cells and bone marrow-derived macrophages

Primary mouse SMCs were isolated from the aortas of 6–8 weeks old C57BL/6J male mice, as previously described [16]. SMCs were grown to confluence in DMEM (Gibco) supplemented with 10% fetal bovine serum (FBS, Gibco), 100 U/mL penicillin, and 100 µg/mL streptomycin at 37 °C in 5% CO_2. The experiments were performed with SMCs between passages 2 and 10.

To generate bone marrow-derived macrophages (BMDMs), bone marrow was harvested from the femurs and tibias of mice, as previously described [17]. The cells were cultured in macrophage medium, consisting of DMEM supplemented with 10% FBS, 1% penicillin/streptomycin, and 20 ng/mL of murine M-CSF. Cells were maintained at 37 °C and 5% CO_2, with a complete medium change after three days. Following a total of seven days of differentiation, the adherent cells were ready for subsequent experiments.

For the treatment of SMCs with BMDM conditioned medium, primary SMCs were serum-starved in DMEM containing 0.3% FBS, 100 U/mL penicillin, and 100 µg/mL streptomycin for 48 h. In the meantime, BMDMs were first primed with 20 ng/mL IFNγ overnight, followed by a 4-hour LPS stimulation (100 ng/mL). The IFNγ/LPS treated and control BMDMs were then thoroughly washed with PBS 4 times. Fresh DMEM containing 0.3% FBS, 100 U/mL penicillin, 100 µg/mL streptomycin and 10ng/mL M-CSF were added to the BMDMs. After a 24-hour incubation period, the conditioned media was harvested and centrifuged at 1000 g for 5 min to remove any cell debris. Subsequently, the SMCs were exposed to the conditioned media, which was prepared from equal numbers of BMDMs.

Human macrophage and neutrophil differentiation and conditioned media collection

Human macrophage-like cells were differentiated from the THP-1 monocyte cell line (ATCC, TIB-202) following a protocol adapted from Baxter et al. [18]. THP-1 cells were maintained in RPMI-1640 medium supplemented with 10% FBS. To induce differentiation into macrophage-like cells, THP-1 cells were treated with 100 nM phorbol 12-myristate 13-acetate (PMA) for 24 h, followed by 24 h of resting period in PMA-free growth medium. To generate the inflammatory secretome, differentiated macrophages were primed with 20 ng/mL IFNγ overnight, followed by stimulation with 100 ng/mL LPS for 4 h. Cells were washed three times with PBS to ensure the removal of exogenous stimuli. The medium was then replaced with human vascular SMC basal medium

(M231500, ThermoFisher Scientific) supplemented with 0.5% FBS. After 24 h of incubation, the conditioned medium was collected, centrifuged at 1000 g for 5 min to remove cellular debris, and the resulting supernatant was used for SMC treatment.

Human neutrophil-like cells were differentiated from the HL-60 myeloid leukemia cell line (ATCC, CCL-240) following the protocol described by Babatunde et al. [19]. HL-60 cells were cultured in RPMI-1640 medium supplemented with 2% FBS, 1.3% DMSO, and 2% Nutridoma (11363743001, Sigma-Aldrich) for 5 days. To induce an inflammatory phenotype, the differentiated neutrophil-like cells were stimulated with 100 nM PMA for 6 h. After stimulation, cells were washed three times with PBS to ensure the complete removal of PMA. The medium was then replaced with SMC basal medium supplemented with 0.5% FBS. After 24 h of incubation, the conditioned medium was collected and centrifuged at 1000 g for 5 min to remove cellular debris.

Primary human saphenous vein SMCs were serum-starved in human vascular SMC basal medium containing 0.5% FBS for 24 h. The SMCs were then incubated with either macrophage-derived or neutrophil-derived conditioned media for an additional 24 h before harvesting for downstream analysis.

Western blotting

Cells or tissues were lysed in RIPA buffer (R0278, Sigma-Aldrich) containing protease and phosphatase inhibitors (Halt Cocktail, ThermoFisher Scientific). Protein extracts were loaded and separated by SDS-PAGE and then transferred to polyvinylidene fluoride membranes. The membranes were blocked with 5% skim milk, and incubated overnight at 4 °C with the following primary antibodies: anti-Phospho-YAP (Ser127) (13008, Cell Signaling Technology; 1:1000), anti-YAP (14074, Cell Signaling Technology, 1:1000), anti-Phospho-YAP (Ser397) (13619, Cell Signaling Technology; 1:1000), anti-SM22α (36090, Cell Signaling Technology; 1:1000), anti-MYH11 (ab133567, Abcam; 1:1000), anti-pan-TEAD (13295, Cell Signaling Technology, 1:1000), anti-α-smooth muscle actin (19245, Cell Signaling Technology, 1:1000), anti-β-actin (A5441, Sigma-Aldrich, 1:5000), followed by HRP (horseradish peroxidase)-labeled secondary antibody (Jackson ImmunoResearch, 1:5000).

RT-qPCR

Total RNA was extracted from cultured cells using PureLink™ RNA Mini Kit (12183018 A, ThermoFisher Scientific) according to manufacturer's protocols. One microgram total RNA was used for the first-strand cDNA synthesis followed by real-time RT-qPCR (polymerase chain reaction). Primer sequences used were listed in Supplemental Table S1.

Collagen gel contraction assay

Collagen gel contraction assay was performed as described previously [20]. Briefly, a collagen suspension (1.5 mg/mL) containing trypsin-digested SMCs was cast in one well of a 24-well culture plate. The suspension contained 0.6 ml (1.5×10^5 cells). The gel was allowed to polymerize for 30 min at 37 °C. Once polymerized, the gel was carefully detached from the culture well using a pipette tip and immediately exposed to conditioned media at 37 °C. The gels were incubated for 24 h. The collagen gel size change was measured at various times using a ruler and quantified using Fiji image analysis software.

Scratch wound healing assay

1.5×10^5 SMCs were seeded into a 24-well plate and allowed to grow until they form a confluent monolayer. The wound was created by using a pipette tip. After 24 h, the cells were then observed under a microscope and images were captured to measure the extent of wound closure by using Fiji image analysis software.

Co-immunoprecipitation

Cells were lysed in Pierce IP Lysis Buffer (Thermo Scientific, 87787) and co-immunoprecipitation experiments were performed using SureBeads magnetic beads (Biorad, 1614013) as per the manufacturer's protocol. In brief, Protein A magnetic beads were washed in TBST, incubated with anti-YAP (14074, Cell Signaling Technology, 1:1000) or rabbit IgG isotype control (Thermo Scientific, 026102) for 30 min at room temperature, and then magnetized and washed three times with TBST. The beads were then incubated with cell lysate overnight at 4 °C. After incubation, the beads were washed three times with TBST, and the immunoprecipitated proteins were eluted in 1x Laemmli buffer and subjected to pan-TEAD immunoblotting.

IL-1β inhibition and functional assays

siRNA knockdown

Mouse macrophage cell line RAW 264.7 (TIB-71, ATCC) was transfected with three siRNAs targeting different regions of *Il1b* mRNA (si-Il1b, mm.Ri.Il1b.13, IDT) or scrambled negative control siRNA (si-Control, 51-01-19-09, IDT). Following transfection, cells were primed with 20 ng/mL IFNγ overnight and stimulated with 100 ng/mL LPS for 4 h to induce *Il1b* expression. Knockdown efficiency was examined via RT-qPCR. Mouse bone marrow-derived macrophages (BMDMs) were similarly transfected with si-Il1b or si-Control and stimulated. Following four PBS washes to remove exogenous stimuli, fresh medium was added, and conditioned medium was collected after 24 h. Primary mouse aortic SMCs were

treated with this conditioned medium for 24 h prior to gene expression analysis via RT-qPCR.

Antibody neutralization

20 ng/mL recombinant IL-1β (575104, BioLegend) or BSA control was premixed with anti-IL-1β neutralizing antibody (503513, BioLegend) or IgG control (400901, BioLegend) for 15 min. The premix was then added to primary mouse aortic SMCs for 24 h. IL-1β activity was assessed by *Ccl2* expression via RT-qPCR. Mouse BMDM conditioned medium was premixed with neutralizing antibody or IgG control as described above before application to SMCs for 24 h.

IL-1 Receptor antagonism

Primary mouse aortic SMCs were pretreated with IL-1 Receptor Antagonist (IL-1RA, 769702, BioLegend) or BSA for 15 min, followed by 20 ng/mL recombinant IL-1β stimulation for 24 h. IL-1β activity was examined by *Ccl2* expression via RT-qPCR. Mouse BMDM conditioned medium was premixed with IL-1RA or BSA for 15 min and added into SMCs for 24 h.

Statistical analysis

Results are presented as mean ± standard deviation. To assess normality, Shapiro-Wilk normality tests were conducted on the data. If the data did not exhibit a normal distribution, they were log2-transformed and retested for normality. For normally distributed data, a two-tailed Student t test was used for comparison between two conditions. For non-normally distributed data after transformation, a Mann-Whitney U nonparametric test was employed. For comparisons of ≥ 3 means, a one-way ANOVA with a Tukey post hoc test was used for normally distributed data, while a Kruskal-Wallis nonparametric test was used for non-normally distributed data. For comparisons of how a response is affected by two factors, a two-way ANOVA followed by Sidak multiple comparisons was performed. Statistical analyses were conducted using GraphPad Prism 9.0 (GraphPad Software, Inc). Experiments were repeated as indicated, and differences with $p < 0.05$ were considered statistically significant.

Results

Vein wall cellular landscape in female and male mouse DVT

We began to investigate SMC phenotypic change during DVT development by performing IVC ligation or sham surgery in age (8 to 12 weeks) matched male and female C57BL/6J mice. 24 h after the procedure, when blood clots were visibly formed but not yet firmly attached to the vein wall, IVC tissues were collected, and blood clots were removed. Single-cell suspensions from 6 DVT-adjacent IVCs and suspensions from 6 sham IVCs were pooled to generate the experimental sample and control sample, respectively. From each pooled sample, 10,000 cells were subjected to scRNA-seq.

Based on the transcriptomic profiles, cells were separated into different clusters on the Minimum-Distortion Embedding (MDE) plot. At 24-hour post-ligation, the vein wall from both males and females contained 8 distinct cell types: smooth muscle cells (SMCs), fibroblasts (FBs), endothelial cells (ECs), neutrophils (Neus), monocytes/macrophages (Mo/Mϕs), T&NK cells, B cells and dendritic cells (DCs) (Fig. 1A). We also detected a very low number of Schwann cells, however, excluded them from further analyses due to their low abundance. Although the relative changes in cell distributions appeared to be slightly different in males and females, the vein wall of both sexes responded to DVT induction with increased percentage of neutrophils but decrease of SMCs, ECs, FBs and Mo/Mϕs (Fig. 1B and Supplemental Table S2). Differentially expressed genes (DEGs) and gene ontology (GO) analysis showed that, in both female and male vein walls, DVT induced higher expression of inflammatory response and leukocyte migration associated genes including *Nos2*, *Cd14*, *Tnf*, *IL-1β*, *Mmp9*, and *Cxcr2*. In contrast, DVT suppressed the expression of genes associated with extracellular matrix organization and SMC contractility including *Eln*, *Col1a1*, *Col3a1*, *Myh11*, and *Cnn1* (Fig. 1C-E).

Cell-cell communications within the vein wall

We next investigated intercellular mechanisms that may govern vein wall remodeling during DVT by analyzing the integrated scRNA-seq dataset using the R package CellChat (Version 2.1). Compared to sham, DVT vein wall showed enhanced intercellular communications from neutrophils and macrophages to vascular cells (ECs, SMCs and FBs) in both sexes, although this effect was more profound in males (Fig. 2A). Similarly, DVT increased EC-to-EC communications in both sexes, with a more significant increase observed in males (Fig. 2A). When examining the signaling pathways from macrophages to SMCs, DVT enhanced signals for SPP1, IL1, GALECTIN, TWEAK, SEMA3, LIGHT, VEGF, and TGFβ in both sexes. In contrast, sham-group veins primarily featured pathways mediated by BMP, IGF, PROS, PTPR, GRN, and GAS (Fig. 2B). A shift in specific signaling pathway was also observed in neutrophil-to-SMC signaling (Fig. 2B). Further examination of the ligand-receptor pairs showed that the communication probabilities of inflammation related ligand-receptor pairs, for example Spp1-Cd44, Il1b-(Il1r1 + Il1rap) and Lgals9-P4hb, were enhanced, while anti-inflammation or wound healing associated ligand-receptor interaction such as Grn-Sort1 and Bmp2-(Bmpr1a+Bmpr2) were decreased in DVT vein walls (Fig. 2C).

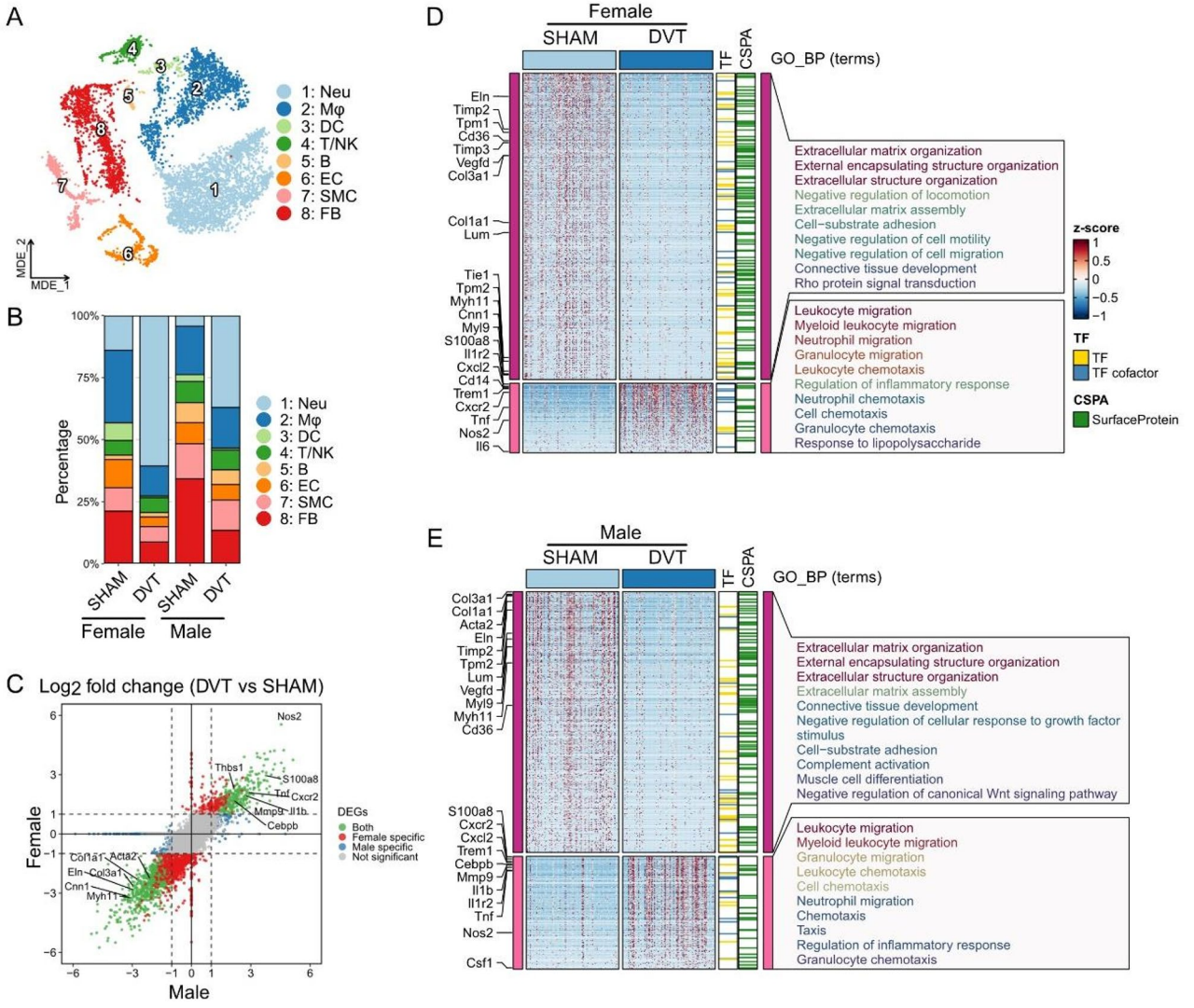

Fig. 1 Identification of cell populations in the vein wall of a murine deep vein thrombosis (DVT) model. **A** Minimum-Distortion Embedding (MDE) plot of cell clusters identified in the vein wall (male, female, SHAM, and DVT data combined). Neu: neutrophil, DC: dendritic cell, T/NK: T and natural killer cells, B: B cell, EC: endothelial cell, SMC: smooth muscle cell, FB: fibroblast. **B** The percentages of cell populations in each group. **C** Scatter plot of DVT vs. SHAM log2 fold change of gene expression in male and female groups. DEG: differentially expressed gene. **D** & **E** Heatmaps and gene ontology biological process (GO_BP) enrichment analysis of differentially expressed genes in male or female groups (DVT vs. SHAM, false discovery rate < 0.05, log2 fold change > 1 or < -1). TF: transcription factor, CSPA: Cell Surface Protein Atlas

Smooth muscle cell phenotypic switching in DVT

We observed 3 major sub-populations of SMCs in the vein wall of both sexes (Fig. 3A), SMC-1 was enriched in expression of genes related to cell migration, ECM organization and inflammation response like *Il1r1*, *Il1r2*, *Cxcl12,* and *Ccl5*, and SMC-3 was likely contractile SMCs which enriched with expressions of muscle structure development associate genes including *Tpm2*, *Acta2,* and *Tagln*. SMC-2 was an intermediate state between SMC-1 and SMC-3, with high expression of organelle assembly genes (Fig. 3B). In both sexes, DVT induction altered the distribution of SMC sub-populations by increasing the percentage of SMC-1 while decreasing contractile SMC-3 (Fig. 3C). Trajectory (Fig. 3A), RNA velocity (Fig. 3D) and pseudotime (Fig. 3E) analyses showed that DVT caused a transition from SMC-3 toward SMC-1 in the vein wall. Predicted dynamic gene expression changes during the transition revealed a reduction in smooth muscle contractile genes (*Acta2*, *Cnn1*, *Tagln,* and *Tpm2*) but an increase in stimulus response genes (*S100a10*, *Egfr,* and *Il1r1*). Gene ontology analysis of these altered genes showed that pathways such as "Muscle system process" and "Muscle contraction" were repressed, however, "Response to growth factor", "Response to endogenous stimulus" and "Cell migration" pathways were induced along the evolution trajectory (Fig. 3F).

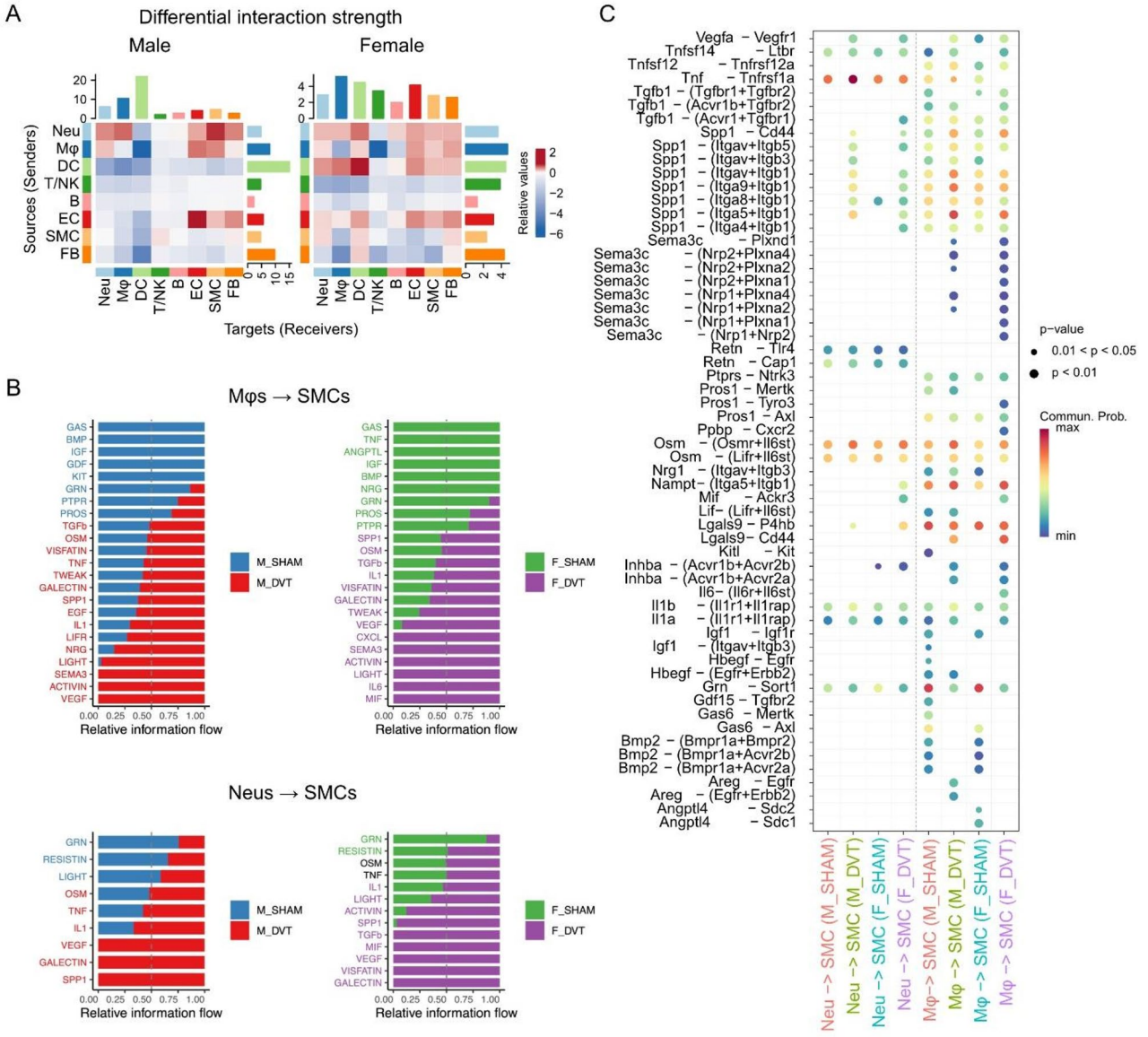

Fig. 2 Cell-cell communication in the vein wall. **A** Heatmap of differential interaction strength in the DVT group compared to the SHAM group. The top bar plot represents the sum of incoming signals, while the right bar plot represents the sum of outgoing signals. Red (or blue) represents increased (or decreased) signaling in DVT compared to SHAM. Relative value = the interaction strength from source to target in DVT group – the interaction strength from source to target in SHAM group. **B** Relative information flow of each signaling pathway from macrophages (Mφs) to smooth muscle cells (SMCs) or from neutrophils (Neus) to SMCs in SHAM and DVT groups. **C** Communication probability of ligand-receptor pairs mediating communications between Neus-SMCs or Mφ-SMCs

M1-like pro-inflammatory macrophages expand in DVT

Having observed enhanced macrophage-to-SMC communication in DVT, we further analyzed macrophage populations in the scRNA-seq data. As shown in Supplemental Figure S1, three macrophage sub-populations were noted. Mϕ-1 was characterized by high expression of gene related to regulation of immune response, likely pro-inflammatory or M1-like macrophages; Mϕ-3 enriched with genes related to endocytosis and locomotion, likely anti-inflammatory or M2-like macrophages; Mϕ-2 was an intermediate stage between Mϕ-1 and Mϕ-3. In both males and females, DVT increased the expression of pro-inflammatory genes and the percentage of Mϕ-1 compared to the sham group, although this pro-inflammatory shift was more pronounced in the vein wall of male mice.

Macrophage-SMC communications in vitro

To investigate the signaling mechanism underlying macrophage-to-SMC communication, we conducted bulk RNA sequencing of SMCs after treating them with conditioned media from naïve macrophages (M0-like)

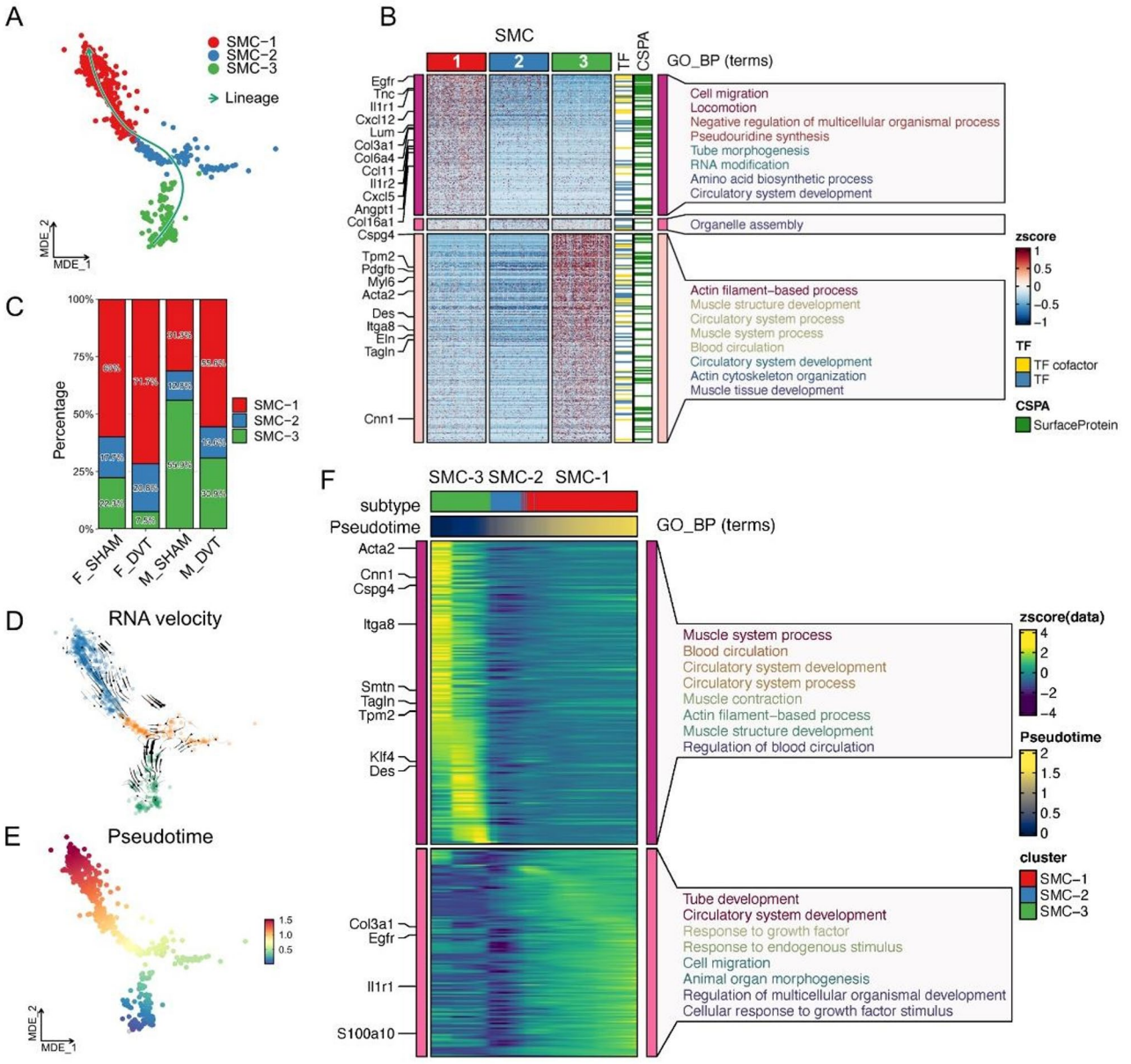

Fig. 3 Phenotypic switching of SMCs during DVT. **A** Subtypes of SMCs in the vein wall. The green line shows the inferred directed trajectory of cell transition. **B** Heatmap of molecular and GO_BP signatures for each SMC sub-cluster. **C** The percentages of SMC sub-clusters in SHAM or DVT groups. **D** RNA velocity analysis of SMC sub-clusters. The arrow's direction indicates the predicted future state of a cell, while its length reflects the speed of transcriptional change. **E** Pseudotime predicted based on RNA velocity analysis. **F** Gene expression changes along the pseudotime axis

or inflammatory M1-like macrophages (polarized with LPS+IFNγ). Principal component analysis (PCA) showed that the transcriptomic profiles of SMCs treated with M1-like conditioned media (referred to as M1-CM) were drastically different from those of SMCs treated with M0-CM or SMCs cultured in regular growth medium (referred to as Reg) (Fig. 4A). DGE analysis showed 1423 up-regulated and 1427 down-regulated genes in M1-CM group (threshold: $p < 0.01$, log2 fold change > 1 or < -1) compared to M0 group (Fig. 4B). KEGG gene set enrichment analysis (GSEA) suggested that the up-regulated genes were mostly enriched in inflammatory response pathways (representative genes: *Ccl2*, *Il6*, *Nos2,* and *Lgals3*) such as TNF signaling pathway, Toll-like receptor signaling pathway, NF-κB signaling pathway, chemokine signaling pathway, as well as apoptosis pathway (*Fas*, *Tnfsf10*, *Casp7*, *Casp10,* and *Ripk1*); while down-regulated genes were related to Cardiac muscle contraction (*Myh11*, *Smtn*, *Acta2*, *Tpm1,* and *Tpm2*), Cell cycle (*Cdk1*, *Cdc7*, *Mki67,* and *Pcna*), Wnt, and Hippo signaling pathway (Fig. 4B&C). Moreover, significant reductions of protein level of MYH11 and mRNA levels of

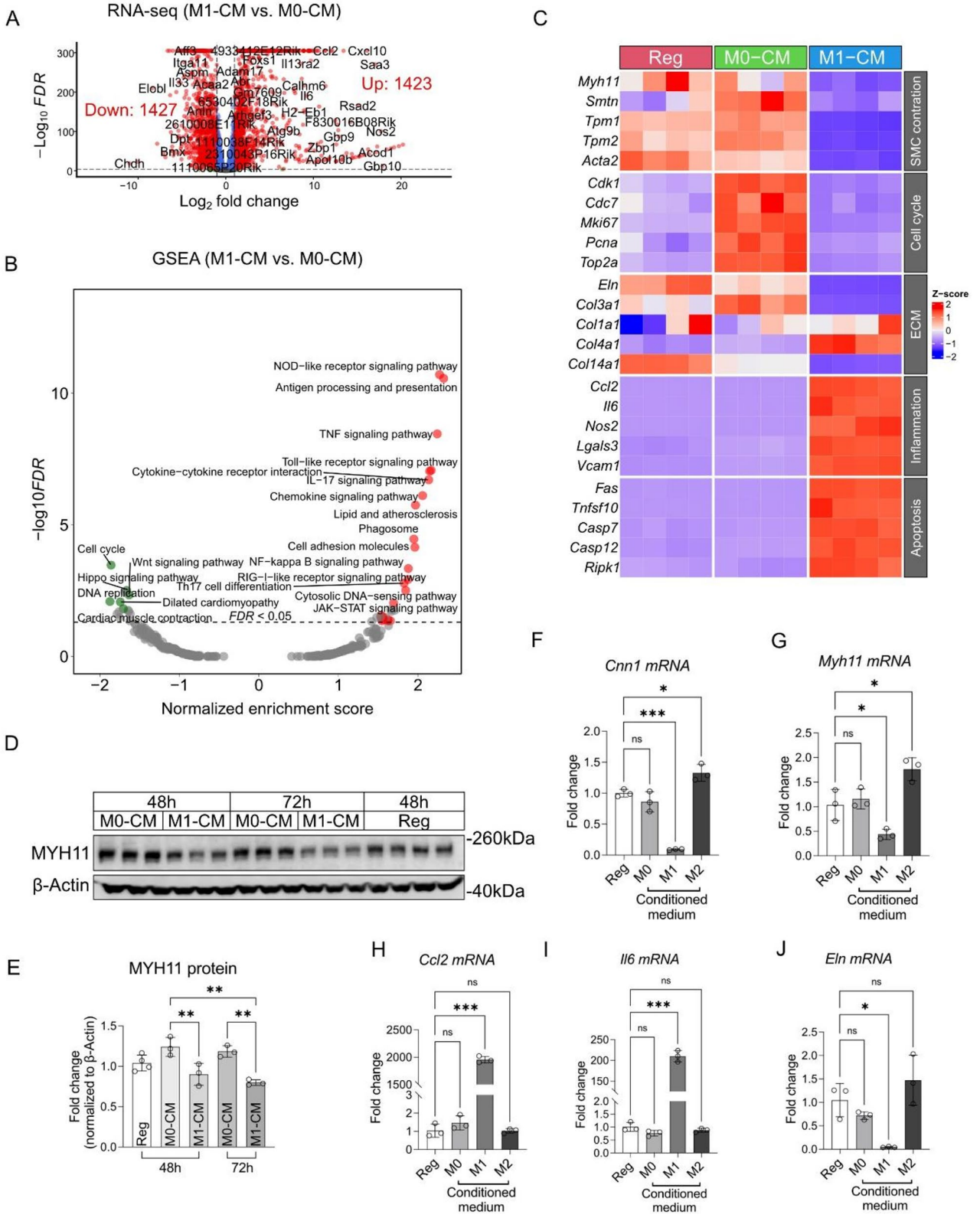

Fig. 4 Macrophage-SMC communications in vitro. **A** Volcano plot of differentially expressed genes (DEGs) of bulk RNA-seq of mouse primary SMCs treated with indicated conditioned media from bone marrow-derived macrophages (BMDMs) for 24 h. **B** Gene set enrichment analysis (GSEA) of DEGs using KEGG pathway terms. **C** Heatmap showing the expression of representative genes from dysregulated pathways. **D** Western blot of MYH11 in mouse primary SMCs treated with indicated conditioned media. **E** Quantification of the Western blot in (D). **F-J** RT-qPCR validation of differentially expressed genes identified by bulk RNA-seq. Data in (E-J) are presented as mean ± SD. One-way ANOVA is performed. *$p < 0.05$, **$p < 0.01$, ***$p < 0.001$

Cnn1, *Eln,* and *Myh11* in M1-CM group were validated by Western blotting and RT-qPCR, respectively (Fig. 4D-G&J), which was consistent with our scRNA-seq analysis showing decreased contractile SMC population (SMC-3) in the DVT vein wall (Fig. 3C). RT-qPCR of *Ccl2* and *Il6* also confirmed the stimulation of inflammation in SMCs treated with M1-CM (Fig. 4H&I).

Phenotypic switching of human venous SMCs in response to the inflammatory secretome

To enhance the human relevance of our findings and address potential differences between arterial and venous SMCs, we repeated several key mechanistic studies using primary SMCs isolated from human saphenous veins. The identity and purity of human venous SMCs were validated by immunofluorescence staining for the contractile markers calponin-1 and SM22α (Fig. 5A).

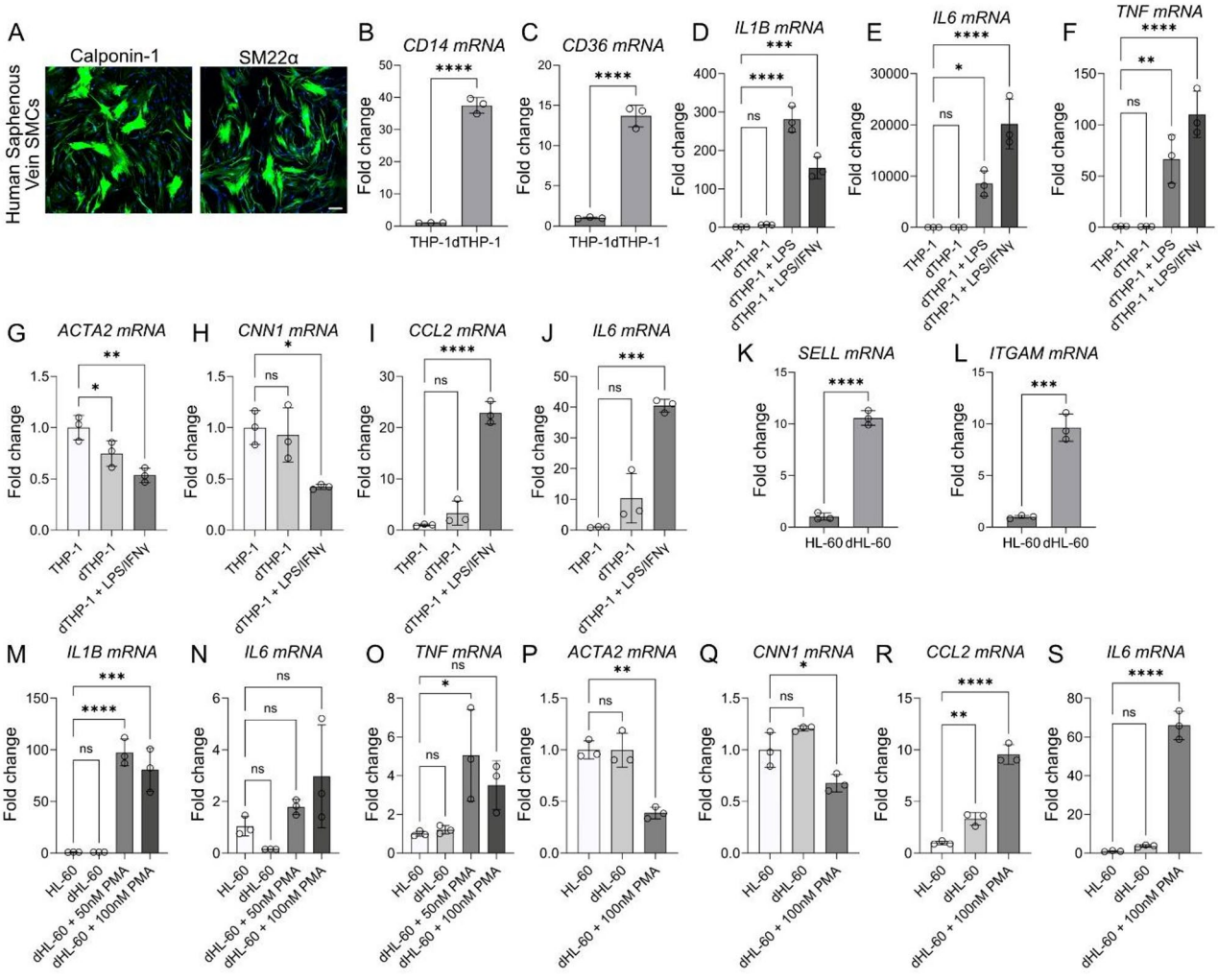

Fig. 5 Human venous SMC responses to macrophage or neutrophil secretome. **A** Validation of human saphenous vein SMCs identity and purity via immunofluorescence staining for the contractile markers calponin-1 or SM22α (green). Nuclei are counterstained with DAPI (blue). Scale bar = 100 μm. **B** & **C** THP-1 cells were differentiated into macrophage-like cells (dTHP-1) by treatment with 100 nM phorbol 12-myristate 13-acetate (PMA) for 24 h, followed by a 24-hour resting period in PMA-free medium. Expression of macrophage markers *CD14* (**B**) and *CD36* (**C**) was validated by RT-qPCR. **D**-**F** Induction of an inflammatory state in dTHP-1 cells using 100 ng/mL LPS and 20 ng/mL IFNγ. The inflammatory phenotype was assessed by the expression of *IL1B* (**D**), *IL6* (**E**), and *TNF* (**F**) via RT-qPCR. **G**-**J** Human saphenous vein SMCs from donor #1 were treated with conditioned media from undifferentiated THP-1 cells, dTHP-1 cells, or LPS/IFNγ-stimulated dTHP-1 cells. Expression of the contractile markers *ACTA2* (**G**) and *CNN1* (**H**), and inflammatory markers *CCL2* (**I**) and *IL6* (**J**) was examined by RT-qPCR. **K** & **L** Differentiation of HL-60 cells into neutrophil-like cells (dHL-60) using medium supplemented with 2% FBS, 1.3% DMSO, and 2% Nutridoma for 5 days. Successful differentiation was confirmed by the expression of *SELL* (L-selectin) (**K**) and *ITGAM* (CD11b) (**L**) via RT-qPCR. **M**-**O** Induction of an inflammatory state in dHL-60 cells using phorbol 12-myristate 13-acetate (PMA). Activation was validated by the increased expression of *IL1B* (**M**), *IL6* (**N**), and *TNF* (**O**) via RT-qPCR. **P**-**S** Human saphenous vein SMCs from donor #1 were treated with conditioned media from undifferentiated HL-60 cells, dHL-60 cells, or PMA-activated dHL-60 cells. Expression of contractile markers *ACTA2* (**P**) and *CNN1* (**Q**), and inflammatory markers *CCL2* (**R**) and *IL6* (**S**) was examined by RT-qPCR. Data in (**B**-**S**) are presented as mean ± SD. Student t test is performed in (**B**&**C**, **K**&**L**), one-way ANOVA followed by a post-hoc test is performed in (**D**-**J**, **M**-**S**). *$p < 0.05$, **$p < 0.01$, ***$p < 0.001$, ****$p < 0.0001$

To investigate the effects of human macrophage-derived signaling, we utilized differentiated THP-1 cells (dTHP-1), which were validated by elevated expression of *CD14* and *CD36* (Fig. 5B&C). An inflammatory state of dTHP-1 cells was induced using 100 ng/mL LPS and 20 ng/mL IFNγ, and confirmed by significant increases in *IL1B*, *IL6*, and *TNFα* expression (Fig. 5D-F). Human saphenous vein SMCs (from two independent donors) responded to the inflammatory human macrophage secretome with significant downregulation of the contractile genes *ACTA2* (donor #1) and *CNN1* (and *TAGLN* in donor #2), along with upregulation of the inflammatory markers *CCL2* and *IL6* (Fig. 5G-J and Supplemental Fig. S2A-E).

Given that neutrophils are the predominant leukocyte infiltrating the acute DVT vein wall, we further examined the impact of neutrophil-derived factors using HL-60-derived neutrophil-like cells. Successful differentiation was confirmed by the elevated expression of *SELL* (L-selectin) and *ITGAM* (CD11B) (Fig. 5K&L), and an inflammatory state was induced via PMA activation, confirmed by *IL1B*, *IL6*, and *TNFα* upregulation (Fig. 5M-O). Similar to the macrophage results, human venous SMCs treated with inflammatory neutrophil-derived conditioned media exhibited a marked decrease in contractile gene expression (*ACTA2* and *CNN1*) and an induction of inflammatory genes (*IL6* and *CCL2*) across both donors (Fig. 5P-S and Supplemental Fig. S2F-I).

Functional analyses of macrophage-conditioned medium-treated SMCs

To determine whether macrophages alter the functions of SMCs, we first measured contractibility using collagen gel contraction assay. M1-CM treatment significantly reduced SMC's ability to contract, reflected by their diminished ability to shrink the collagen gel (Fig. 6A). We next assessed SMC migration using the scratch assay. As shown Fig. 6B, M0-CM significantly promoted scratch wound closure. M1-CM slightly hindered SMC migration in the scratch assay, albeit insignificantly.

Pro-inflammatory macrophages decreases YAP signaling in SMCs

As bulk RNA-seq revealed M1-CM reduced the Hippo signaling pathway in SMCs (Fig. 4B), we examined Yes-associated protein (YAP), the central effector of the Hippo signaling pathway, focusing on YAP phosphorylation (S127 and S397) in CM-treated SMCs. M1-CM increased phosphorylation of YAP S127 and S397, peaked in 3–12 h and 1–6 h, respectively (Fig. 7A-C). After 24 h of CM treatment, total YAP level was significantly lower in the M1-CM group compared to the M0-CM group (Fig. 7D). Since M1-CM did not change the mRNA level of *Yap1* (Fig. 7E), we hypothesized that the reduced abundance of total YAP was due to hyperphosphorylation and subsequent protein degradation. Consistent with the decreased total YAP level, YAP-TEAD target genes (*Amot*, *Tgfb2*, *Tgfb3*, *Ccn1*, *Ccn4* and *Bmp4*) were also reduced in M1-CM group (Fig. 7E). Notably, M1-CM altered the mRNA expression of YAP binding partners, specifically reducing *Tead2-4* expression but increasing *Tead1* (Fig. 7E). Co-IP assay also showed reduced YAP-TEAD interaction (Fig. 7F), suggesting YAP-TEAD transcription activity was inhibited in M1-CM treated SMCs. To further examined whether YAP mediates the downregulation of contractile genes by M1-CM, we applied PY-60, a small molecule that activates YAP transcriptional activity [21], to SMCs treated with M0- or M1-CM. RT-qPCR result demonstrated that PY-60 robustly promoted *Cnn1* gene expression in both M0- and M1-CM groups (Fig. 7G).

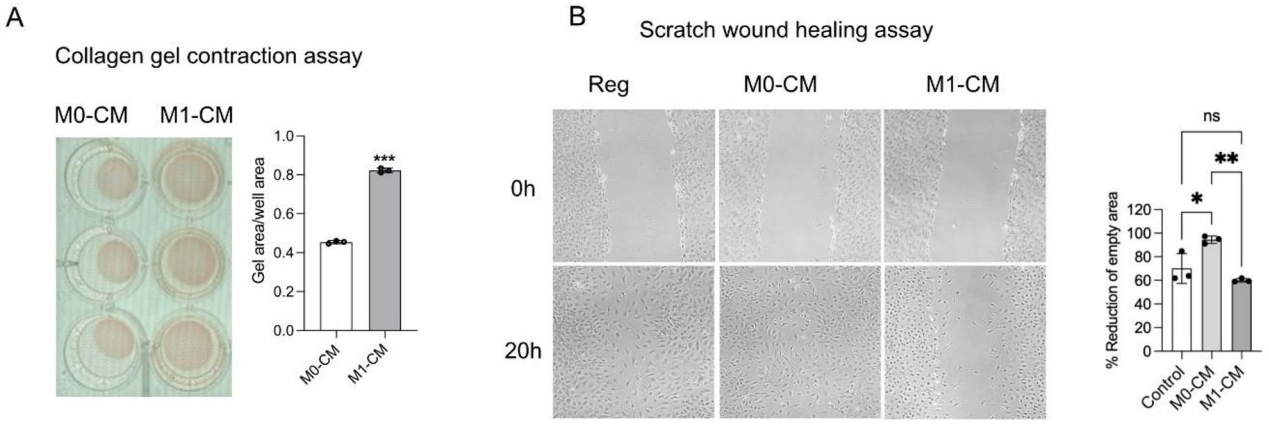

Fig. 6 Functional analyses of SMCs treated with BMDM-conditioned media. **A** Representative images and quantification of collagen contraction assay of primary mouse SMCs treated with BMDM conditioned media for 24 h. **B** Representative images and quantification of scratch wound healing assay of primary SMCs treated with BMDM conditioned media. Data in are presented as mean ± SD. Student t test is performed in (**A**). One-way ANOVA is performed in (**B**). *$p < 0.05$, **$p < 0.01$, ***$p < 0.001$

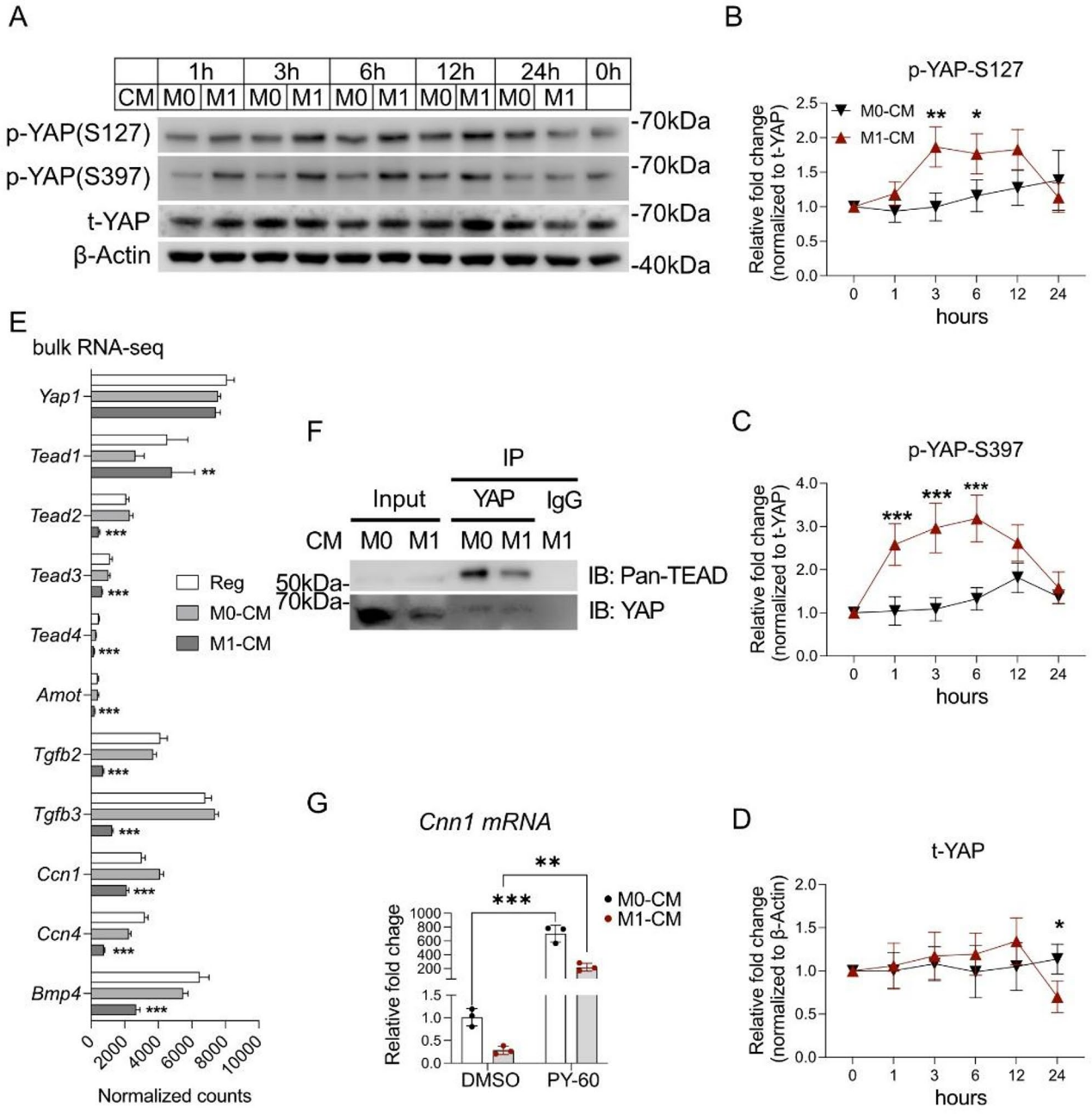

Fig. 7 YAP signaling in macrophage conditioned media-treated SMCs. **A**-**D** Time course of phospho-YAP (S127 or S397) and total YAP in mouse primary SMCs treated with M0 or M1- like BMDM conditioned medium (CM). **E** Normalized counts of genes associated with YAP-TEAD pathway in SMCs from bulk RNA-seq data. **F** Co-immunoprecipitation (Co-IP) of YAP and pan-TEAD in SMCs treated with M0 or M1- like BMDM conditioned medium. **G** RT-qPCR of *Cnn1* in SMCs treated with BMDM-CM or YAP-TEAD pathway activator PY-60 for 24 h. Data in are presented as mean ± SD. Two-way ANOVA is performed in (**B-D**) & (**G**). *$p < 0.05$, **$p < 0.01$, ***$p < 0.001$

DVT decreases YAP signaling in the vein wall

To evaluate whether YAP signaling was altered by DVT, we analyzed the vein walls 24 h after stasis DVT induction or sham surgery by Western blotting. We found significant reduction in phosphor-YAP (S127), total YAP, and pan-TEAD in the DVT group, along with markedly diminished levels of contractile protein MYH11 and α-SMA (Fig. 8A&B). Immunostaining of vein wall cross-sections confirmed the reduction of α-SMA, phospho- and total YAP in the DVT group (Fig. 8C&D). Moreover, YAP was predominantly decreased in venous SMCs (Fig. 8C). To further clarify the temporal dynamics of YAP signaling in vivo, we examined the vein wall at the 6-hour time point, representing the onset of luminal clot formation. At this stage, phosphor-YAP (S127) levels remained comparable to sham controls, while

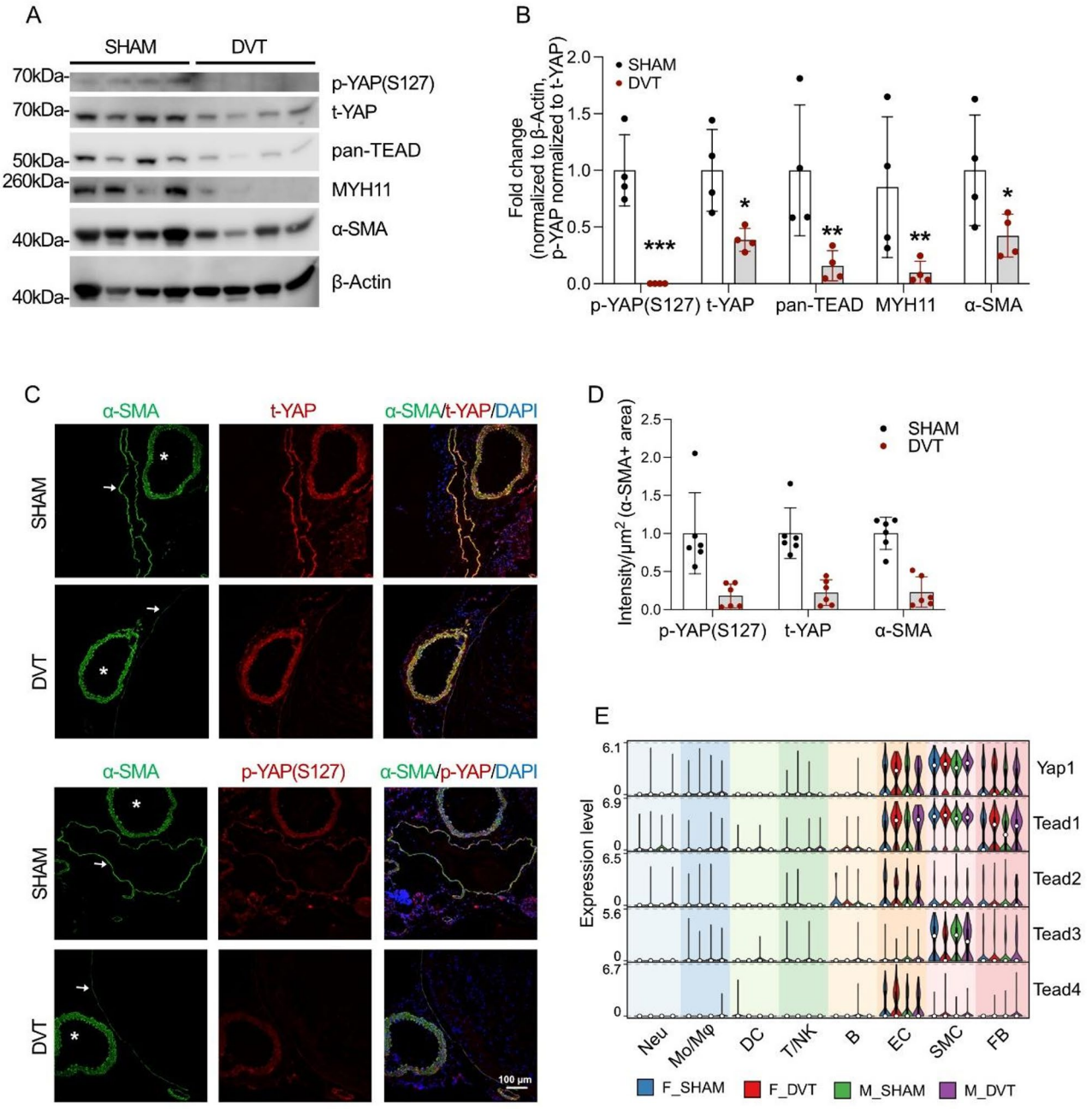

Fig. 8 YAP signaling in the vein wall during DVT. **A**-**B** Western blot and quantification of phospho-YAP(S127), total-YAP, pan-TEAD, MYH11 and α-SMA in vein walls 24 h after SHAM or DVT surgery. **C-D** Representative images and quantification of phospho-YAP(S127), total-YAP, and α-SMA in vein walls 24 h after SHAM or DVT surgery. The white arrow indicates the vein wall; the asterisk indicates the nearby aorta. Scale bar = 100 μm. **E***Yap1* and *Tead1-4* expression and distribution in scRNA-seq data. Data in are presented as mean ± SD. Two-way ANOVA is performed in (B&D). *$p < 0.05$, **$p < 0.01$, ***$p < 0.001$

total YAP and pan-TEAD protein levels already exhibited a downward trend. Additionally, MYH11 showed a downward trend, and α-SMA levels were significantly decreased (Supplemental Fig. S3). Moreover, scRNA-seq analysis showed that SMCs expressed highest level of *Yap1*— along with *Tead1* and *Tead3* — among the major cell types in the vein wall. DVT induction did not change *Yap1* gene expression in SMCs (Fig. 8E), suggesting that transcriptional regulation is unlikely to be the mechanism responsible for the decreased YAP abundance in DVT-affected SMCs.

Macrophages communicate with SMCs via IL-1β

To identify the ligand-receptor pair(s) that mediate the communication between macrophages and SMCs, we conducted a ligand activity analysis using the R package

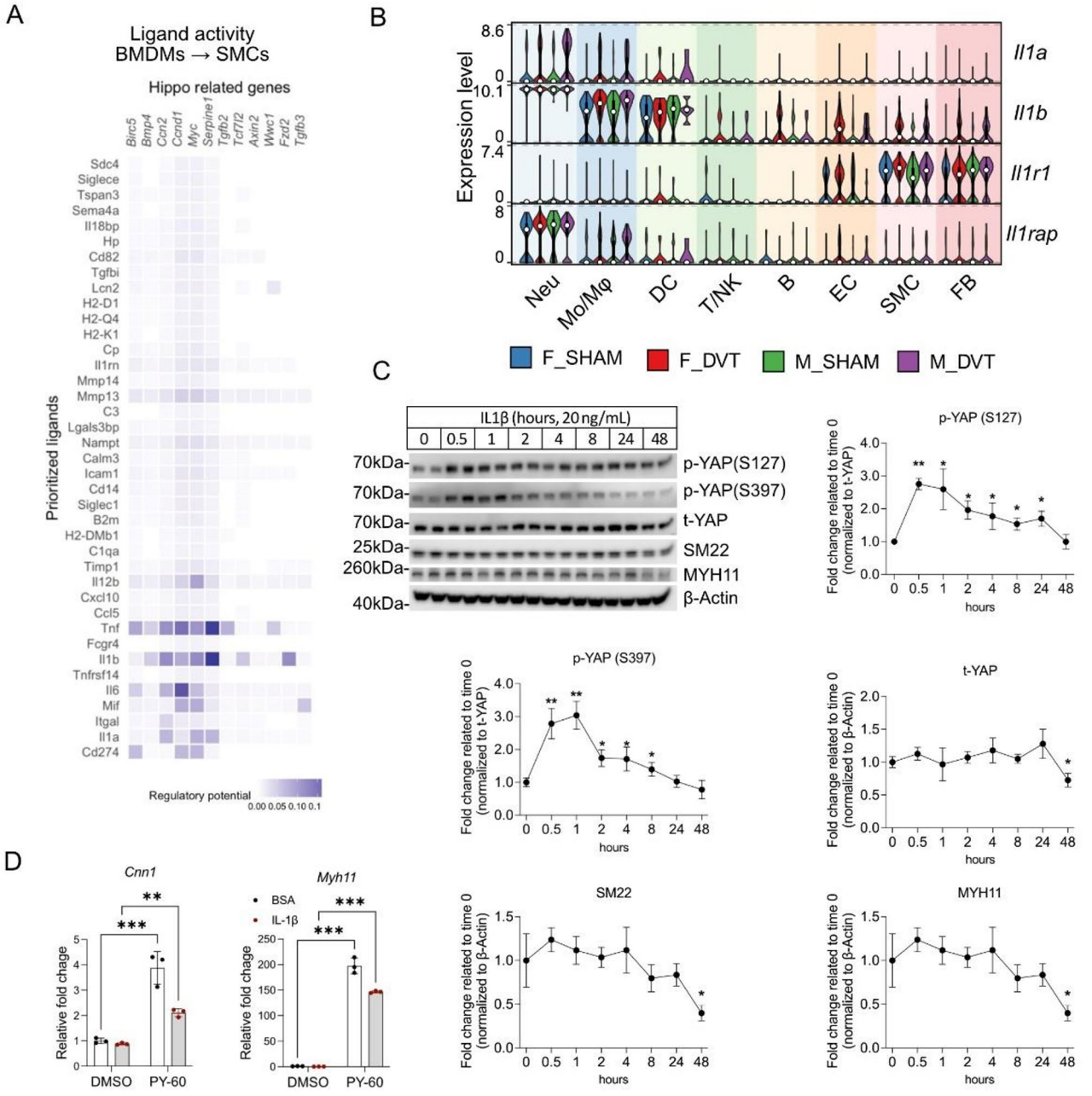

Fig. 9 IL-1β mediates macrophage-SMC communication. **A** Predicted ligand activities mediating BMDM-SMC communication using the NicheNet R package. IFNγ/LPS stimulated BMDM bulk RNA-seq datasets were downloaded from GEO (GSE103958). **B** Expression and cellular distribution of *Il1a*, *Il1b*, *Il1r1* and *Il1rap* in scRNA-seq data. **C** Representative Western blot and quantification of the time course of p-YAP(S127), p-YAP(S397), total-YAP, SM22, and MYH11 protein levels in SMCs challenged with 20 ng/mL recombinant mouse IL-1β. **D** RT-qPCR of *Ccl2* and *Myh11* in SMCs treated with recombinant mouse IL-1β and/or PY-60. Data in are presented as mean ± SD. Two-way ANOVA is performed in (**C**&**D**). *$p < 0.05$, **$p < 0.01$, ***$p < 0.001$

NicheNet, applying it to both the RNAseq data generated in Fig. 4, and publicly available RNAseq data of BMDM treated IFN-γ and LPS (Das A. et al., GSE103958 [22]). Our analysis predicted that BMDM-expressed IL-1β and TNF had the highest potential to regulate the Hippo signaling pathway in SMCs (Fig. 9A). Interestingly, in the vein wall, *Il1b* was highly expressed by macrophages, while *Il1r1* (the major receptor for IL-1β) was enriched in SMCs. The expression levels of *Il1b* and *Il1r1* were elevated by DVT in both sexes (Fig. 9B). To test the role of IL-1β in SMC phenotypic switching, we treated mouse primary SMCs with recombinant mouse IL-1β for various time points. We found that IL-1β significantly increased YAP phosphorylation (S127 and S397) as early as 30 min after treatment (Fig. 9C). Prolonged treatment (48 h) reduced total YAP, as well as the contractile

proteins SM22 and MYH11 (Fig. 9C). The YAP activator PY-60 significantly increased the expression of *Cnn1* and *Myh11* with and without the presence of IL-1β (Fig. 9D).

Impact of IL-1β inhibition on macrophage-SMC crosstalk

To investigate whether IL-1β is required for macrophage-induced SMC phenotypic switching, we attempted to diminish its expression or activity using three separate experimental strategies. We first silenced *Il1b* in macrophages using siRNA achieving an approximately 50% reduction in *Il1b* mRNA levels in RAW 264.7 cells. (Supplemental Fig. S4A). When primary SMCs were treated with conditioned media from siRNA-treated macrophages, although the inflammatory gene *Il6* was decreased, we did not observe a significant rescue in the expression of *Ccl2* or the contractile genes *Acta2* and *Cnn1* (Supplemental Fig. S4B-E).

We next assessed the effect of pharmacological inhibition using an anti- IL-1β neutralizing antibody. Pre-treatment of recombinant IL-1β with the antibody reduced its signaling activity by 40–60%, as measured by *Ccl2* induction in SMCs. Yet, neutralizing IL-1β within the M1-CM secretome was insufficient to significantly ameliorate the downregulation of contractile markers *Myh11* and *Tagln* or the upregulation of *Ccl2* (Supplemental Fig. S4F-I). Similarly, while the IL-1 receptor antagonist (IL-1RA) inhibited recombinant IL-1β activity by 35%, its presence did not significantly alter the phenotypic switching induced by M1-CM (Supplemental Fig. S4J-M).

Discussion

Our unbiased scRNA-seq analysis revealed profound transcriptomic changes in the mouse vein wall 24 h after DVT induction. In addition to the expected neutrophil influx, the thrombus-bearing vein wall exhibited phenotypic switching of SMCs, characterized by diminished expression of contractile genes. Another major early DVT response is the shifting of macrophages toward an inflammatory phenotype. SMC fibrosis is believed to contribute to the thickening and stiffening of the vein wall associated with post-thrombotic syndrome [23, 24], which typically occurs several weeks after DVT induction. Our observation of reduced contractile SMCs in both sexes just 24 h into DVT suggests that SMC phenotypic change begins in the acute phase. This finding points to the potential for early medical interventions to prevent post-thrombotic syndrome.

Several factors released by the luminal thrombi, including PDGF are capable of promoting SMCs switch from the contractile state to synthetic/mesenchymal states. Our scRNA-seq and CellChat analysis identified neutrophils and macrophages that infiltrated the vein wall as novel drivers of SMC phenotypic switching. In full support of this notion, the secretome of inflammatory macrophages drastically altered the gene expression as well as the functions of SMCs in vitro. The bioinformatic analysis of gene expression patterns of SMCs led us to the Hippo signaling pathway. The role of YAP, the central effector of the Hippo signaling, in SMCs has been reported in several arterial diseases. YAP expression was reduced in human aortic aneurysms [25] but increased in vein graft disease [26]. In mouse carotid artery ligation and rat carotid artery balloon injury models, YAP expression was elevated in SMCs, whereas phosphorylated YAP (S127)/total YAP ratio was decreased, in parallel with reduced expression of contractile SMC markers [27]. However, to the best of our knowledge, this study is the first to report that DVT induction triggers a rapid suppression of YAP signaling within the vein wall. Our in vitro data showed that inflammatory macrophages increase YAP phosphorylation (S127 and S397) within 1–12 h, followed by a significant decline in total YAP protein by 24 h. This sequence aligns with the established "phospho-degradon" mechanism, where hyper-phosphorylation targets YAP for proteasomal degradation [28]. Our 24-hour in vivo analysis showed a concurrent reduction in both phosphorylated and total YAP, we suspected this time point represented the "end-stage" of the degradation process. By 24 h post-ligation, the severe depletion of the total YAP pool likely leads to a secondary reduction in the measurable phosphorylated form simply because the substrate is no longer abundant. Our 6-hour in vivo data showed that at this earlier stage, representing the onset of luminal clot formation, total YAP and pan-TEAD levels already exhibit a downward trend while p-YAP levels remain stable. This confirms that the in vivo response follows the same rapid temporal progression observed in vitro, transitioning from early phosphorylation-induced instability to total protein loss. Ultimately, the preservation of contractile gene expression in macrophage-conditioned SMCs upon YAP activation supports its critical pro-differentiation role. Whether pharmacological or genetic manipulation of YAP can prevent SMC phenotypic switching during the acute phase of DVT, and subsequently mitigate long-term fibrotic vein wall remodeling, warrants further investigation.

Clinically, DVT affects both men and women [29]. In mice, IVC ligation causes intraluminal clotting at a similar rate [5]. Consistently, we found in the mouse model, DVT induction triggered generally similar cellular changes in both sexes such as influx of neutrophils and phenotypic switching of SMCs (toward dedifferentiation) and macrophages (toward inflammation). However, subtle sex-dependent responses were noted. For example, the DVT-triggered increase in the expression of pro-inflammatory genes as well as the presence of inflammatory macrophage subtype is more pronounced in the vein

wall of male mice. Future studies are necessary to address this potential sex dimorphism in DVT.

Our study identifies IL-1β as a potent mediator capable of driving SMC phenotypic switching; however, our neutralization and knockdown experiments did not significantly rescue the SMC contractile phenotype when cells were exposed to the full macrophage secretome. It is possible that IL-1β is not the sole driver within the complex inflammatory secretome. Indeed, our scRNA-seq and NicheNet analyses indicated that inflammatory macrophages secrete a wide array of factors, including TNF, IL-6, MIF, and PD-L1, which may function redundantly to drive SMC dedifferentiation. Another possible cause is the incomplete elimination of IL-1β protein or activity from the conditioned media through siRNA knockdown of *Il1b*, neutralizing antibodies, or IL-1RA treatment. This technical "knockdown" failure is amplified by the fact that IL-1β is an exceptionally potent cytokine. Even low residual levels of IL-1β in the conditioned medium may be sufficient to trigger significant cellular responses in SMCs.

There are several limitations associated with the current study. First, our study relies on animal and cell modeling due to the lack of access to tissue from human DVT-affected veins, as DVT is rarely treated with open surgery. Second, the transcriptomic focused scRNA-seq and bulk RNAseq analyses do not provide direct evidence of proteomic changes particularly at the level of post-translational modifications. Furthermore, we acknowledge that this study does not include direct in vivo or ex vivo functional assays to validate the biomechanical impact of SMC dedifferentiation. These investigations were primarily precluded by significant technical difficulties, specifically the structural fragility and limited accessibility of the murine vein wall during the acute phase of thrombosis. As a result, our functional conclusions are largely drawn from in vitro systems.

Conclusions

In this study, we uncovered that SMC phenotypic changes begin during the early phase of murine DVT. The diminished YAP signaling in the vein wall is likely responsible for the reduced contractile gene expression by SMCs within the clot-bearing vein wall. Our work highlights a new role of inflammation in post-thrombotic vein remodeling, which could offer a new treatment direction for DVT patients.

Abbreviations

BMDMs	Bone marrow-derived macrophages
DCs	Dendritic cells
DEGs	Differentially expressed genes
DVT	Deep vein thrombosis
ECs	Endothelial cells
FBs	Fibroblasts
GO	Gene ontology
GSEA	Gene set enrichment analysis
IVC	Inferior vena cava
M1-CM	M1-like conditioned media
Mo/Mφs	Monocytes/macrophages
Neus	Neutrophils
PCA	Principal component analysis
Reg	Regular medium
RT-qPCR	Real-time quantitative polymerase chain reaction
scRNA-seq	Single-cell RNA sequencing
SMCs	Smooth muscle cells
YAP	Yes-associated protein

Supplementary Information

The online version contains supplementary material available at https://doi.org/10.1186/s12964-026-02839-7.

Supplementary Material 1.

Supplementary Material 2.

Acknowledgements

We sincerely thank Dr. Xiaochun Long (Augusta University) for the generous gift of the human saphenous vein smooth muscle cells used in this study. Single-cell RNA sequencing and bulk RNA sequencing was performed at UW Biotechnology Center Gene Expression Center and DNA Sequencing Facility (Research Resource Identifier – RRID: SCR_017757 and SCR_017759).

Authors' contributions

HY conducted the bioinformatic analyses and performed all in vitro experiments. TZ performed animal experiments and prepared the libraries for single-cell and bulk RNA sequencing. JK assisted with the statistical analyses. HY, TZ, and BL drafted the manuscript. All authors read and approved the final version.

Funding

This study was supported by the National Institute of Health (R01HL149404 and R01HL158073 to B. Liu).

Data availability

All data and materials are available from the corresponding author upon reasonable request. The scRNA-seq and bulk RNA-seq data have been deposited in the Gene Expression Omnibus (GEO) under accession numbers GSE326575 and GSE326694, respectively.

Declarations

Ethics approval and consent to participate

Not applicable.

Consent for publication

Not applicable.

Competing interests

The authors declare no competing interests.

Received: 3 September 2025 / Accepted: 21 March 2026
Published online: 27 March 2026

References

1. Heit JA, Silverstein MD, Mohr DN, Petterson TM, Lohse CM, O'Fallon WM, Melton LJ. 3rd: The epidemiology of venous thromboembolism in the community. Thromb Haemost. 2001;86:452–63.
2. Henke PK, Comerota AJ. An update on etiology, prevention, and therapy of postthrombotic syndrome. J Vasc Surg. 2011;53:500–9.
3. Navarrete S, Solar C, Tapia R, Pereira J, Fuentes E, Palomo I. Pathophysiology of deep vein thrombosis. Clin Exp Med. 2023;23:645–54.

4. Diaz JA, Obi AT, Myers DD Jr., Wrobleski SK, Henke PK, Mackman N, Wakefield TW. Critical review of mouse models of venous thrombosis. Arterioscler Thromb Vasc Biol. 2012;32:556–62.
5. Diaz JA, Saha P, Cooley B, Palmer OR, Grover SP, Mackman N, Wakefield TW, Henke PK, Smith A, Lal BK. Choosing a Mouse Model of Venous Thrombosis. Arterioscler Thromb Vasc Biol. 2019;39:311–8.
6. DeRoo E, Zhou T, Yang H, Stranz A, Henke P, Liu B. A vein wall cell atlas of murine venous thrombosis determined by single-cell RNA sequencing. Commun Biol. 2023;6:130.
7. Cao G, Xuan X, Hu J, Zhang R, Jin H, Dong H. How vascular smooth muscle cell phenotype switching contributes to vascular disease. Cell Commun Signal. 2022;20:180.
8. Miano JM, Fisher EA, Majesky MW. Fate and State of Vascular Smooth Muscle Cells in Atherosclerosis. Circulation. 2021;143:2110–6.
9. Elmarasi M, Elmakaty I, Elsayed B, Elsayed A, Zein JA, Boudaka A, Eid AH. Phenotypic switching of vascular smooth muscle cells in atherosclerosis, hypertension, and aortic dissection. J Cell Physiol. 2024;239:e31200.
10. Shankman LS, Gomez D, Cherepanova OA, Salmon M, Alencar GF, Haskins RM, Swiatlowska P, Newman AA, Greene ES, Straub AC, et al. KLF4-dependent phenotypic modulation of smooth muscle cells has a key role in atherosclerotic plaque pathogenesis. Nat Med. 2015;21:628–37.
11. Yap C, Mieremet A, de Vries CJM, Micha D, de Waard V. Six Shades of Vascular Smooth Muscle Cells Illuminated by KLF4 (Krüppel-Like Factor 4). Arterioscler Thromb Vasc Biol. 2021;41:2693–707.
12. Zhao J, Zhang W, Lin M, Wu W, Jiang P, Tou E, Xue M, Richards A, Jourd'heuil D, Asif A, et al. MYOSLID Is a Novel Serum Response Factor-Dependent Long Noncoding RNA That Amplifies the Vascular Smooth Muscle Differentiation Program. Arterioscler Thromb Vasc Biol. 2016;36:2088–99.
13. Zeng Z, Ma Y, Hu L, Tan B, Liu P, Wang Y, Xing C, Xiong Y, Du H. OmicVerse: a framework for bridging and deepening insights across bulk and single-cell sequencing. Nat Commun. 2024;15:5983.
14. Patro R, Duggal G, Love MI, Irizarry RA, Kingsford C. Salmon provides fast and bias-aware quantification of transcript expression. Nat Methods. 2017;14:417–9.
15. Browaeys R, Saelens W, Saeys Y. NicheNet: modeling intercellular communication by linking ligands to target genes. Nat Methods. 2020;17:159–62.
16. Zhai X, Cao S, Wang J, Qiao B, Liu X, Hua R, Zhao M, Sun S, Han Y, Wu S, et al. Carbonylation of Runx2 at K176 by 4-Hydroxynonenal Accelerates Vascular Calcification. Circulation. 2024;149:1752–69.
17. Yang H, Zhou T, Sorenson CM, Sheibani N, Liu B. Myeloid-Derived TSP1 (Thrombospondin-1) Contributes to Abdominal Aortic Aneurysm Through Suppressing Tissue Inhibitor of Metalloproteinases-1. Arterioscler Thromb Vasc Biol. 2020;40:e350–66.
18. Baxter EW, Graham AE, Re NA, Carr IM, Robinson JI, Mackie SL, Morgan AW. Standardized protocols for differentiation of THP-1 cells to macrophages with distinct M(IFNgamma + LPS), M(IL-4) and M(IL-10) phenotypes. J Immunol Methods. 2020;478:112721.
19. Babatunde KA, Wang X, Hopke A, Lannes N, Mantel PY, Irimia D. Chemotaxis and swarming in differentiated HL-60 neutrophil-like cells. Sci Rep. 2021;11:778.
20. Matsumoto H, Moir LM, Oliver BG, Burgess JK, Roth M, Black JL, McParland BE. Comparison of gel contraction mediated by airway smooth muscle cells from patients with and without asthma. Thorax. 2007;62:848–54.
21. Shalhout SZ, Yang PY, Grzelak EM, Nutsch K, Shao S, Zambaldo C, Iaconelli J, Ibrahim L, Stanton C, Chadwick SR, et al. YAP-dependent proliferation by a small molecule targeting annexin A2. Nat Chem Biol. 2021;17:767–75.
22. Das A, Yang CS, Arifuzzaman S, Kim S, Kim SY, Jung KH, Lee YS, Chai YG. High-Resolution Mapping and Dynamics of the Transcriptome, Transcription Factors, and Transcription Co-Factor Networks in Classically and Alternatively Activated Macrophages. Front Immunol. 2018;9:22.
23. Deroo S, Deatrick KB, Henke PK. The vessel wall: A forgotten player in post thrombotic syndrome. Thromb Haemost. 2010;104:681–92.
24. Deatrick KB, Eliason JL, Lynch EM, Moore AJ, Dewyer NA, Varma MR, Pearce CG, Upchurch GR, Wakefield TW, Henke PK. Vein wall remodeling after deep vein thrombosis involves matrix metalloproteinases and late fibrosis in a mouse model. J Vasc Surg. 2005;42:140–8.
25. Arevalo Martinez M, Ritsvall O, Bastrup JA, Celik S, Jakobsson G, Daoud F, Winqvist C, Aspberg A, Rippe C, Maegdefessel L et al. Vascular smooth muscle-specific YAP/TAZ deletion triggers aneurysm development in mouse aorta. JCI Insight 2023, 8.
26. Garoffolo G, Sluiter TJ, Thomas A, Piacentini L, Ruiter MS, Schiavo A, Salvi M, Saccu C, Zoli S, Chiesa M, et al. Blockade of YAP Mechanoactivation Prevents Neointima Formation and Adverse Remodeling in Arterialized Vein Grafts. J Am Heart Assoc. 2025;14:e037531.
27. Wang X, Hu G, Gao X, Wang Y, Zhang W, Harmon EY, Zhi X, Xu Z, Lennartz MR, Barroso M, et al. The induction of yes-associated protein expression after arterial injury is crucial for smooth muscle phenotypic modulation and neointima formation. Arterioscler Thromb Vasc Biol. 2012;32:2662–9.
28. Zhao B, Li L, Tumaneng K, Wang CY, Guan KL. A coordinated phosphorylation by Lats and CK1 regulates YAP stability through SCF(beta-TRCP). Genes Dev. 2010;24:72–85.
29. Prandoni P, Fluharty M, Schellong S, Bounameaux H, Haas S, Mantovani LG, Sholkamy S, Kondo K, Gibbs H, Jing ZC et al. Sex differences in venous thromboembolism outcomes: findings from the GARFIELD-VTE registry. Eur J Intern Med 2025:106492.

Publisher's note